Adam−Gibbs Theory Applied to a Unifying Rheological Model of Crude Oil and Alkanes

Roberto C. Dante,*,† E. Geffroy,† and A. E. Chávez‡

Department of Complex Materials, Instituto de Investigaciones en Materiales, Universidad Nacional Autónoma de México (UNAM), Circuito Exterior S/N, Ciudad Universitaria, Coyoacán, Mexico City, 04510, Mexico, and Department of Chemical Engineering, Facultad de Química, Universidad Nacional Autónoma de México (UNAM), Facultad de Química Conjunto E, Circuito de la Investigación Científica S/N, Coyoacán, Mexico City, 04510, Mexico

Received April 14, 2006. Revised Manuscript Received November 14, 2006

The knowledge of the viscous properties of crude oils is limited by the complexity and variability of the raw materials. Nevertheless, a Weissenberg number, defined by the product of the shear rate and the characteristic time of the considered system, allowed us to scale viscosities of both crude oil and mixtures of alkanes, at different temperatures. This characteristic time has its origins in the reorientation of oligomeric chains of alkanes along the flow direction. This reorientation is associated to an activation energy, which, according to the Adam−Gibbs theory, is correlated to changes of the configurational entropy.

1. Introduction

Crude petroleum is a mixture of several compounds, each with different boiling temperatures that can be separated into a variety of generic fractions by distillation and by fractionation.[1] However, petroleum from different sources exhibits different characteristics, and the behavioral characteristics are often difficult to define with a high degree of precision. There is a wide variation of properties of petroleum, with proportions of different constituents varying largely.[1−3] Thus, some crude oils have higher proportions of the lower boiling constituents, whereas others (such as bitumen, also referred to as natural asphalt) have greater proportions of the higher boiling constituents (often called the "asphaltic components" or "residuum"). However, from a mesostructural point of view, crude oils can be often classified in the general field of suspensions. Nevertheless, not all crude oils are properly suspensions; the term is used here with a certain latitude. This definition is based more on the presence either of asphaltenes or waxes, which can be considered as solid below certain temperatures, rather than inorganic suspended particles such as clay, etc. Crude oil rheology frequently shows a shear thinning behavior in steady shear strain conditions as well as normal stresses.[4] This very complex behavior depends on non-Newtonian contributions due to the colloidal particles.[5] There are two approaches to understand and achieve a general scope of the rheological properties of crude oil: (i) the former consists of reproducing crude oils artificially by mixing several typical compounds of oils in well-known proportions;[6−9] (ii) the latter consists of finding a class of chemically well-defined compounds which can describe at least the main oil characteristics. This piece of work is based on the second choice. The interpretation of the Weissenberg number used to scale viscosities at different temperatures of both crude oil and alkanes is the core of this paper. The Adam−Gibbs theory[10] allows us to correlate the Arrhenius factor, which is part of the characteristic time of the proposed Weissenberg number, with the conformational changes in the aliphatic chains. In this case, thermodynamics will provide the bridge between the macroscopic rheological behavior and the microscopic changes of the conformation of molecules. In this paper, specifically considered are the cases of crude oil samples of the Mexican reservoir of Cantarell, and the blend of *n*-heptadecane (C17) and *n*-eicosane (C20).

2. Adam−Gibbs Theory and Viscoelasticity of Alkanes

The Adam−Gibbs theory was first used to explain the viscoelastic properties in the glass transition range of polymers.[10] Nevertheless, it also applys above 100 °C of the transition

* Corresponding author. Tel.: 0039 0175347328. E-mail address: roberto.dante@itt.com.

† Instituto de Investigaciones en Materiales, Universidad Nacional Autónoma de México (UNAM).

‡ Facultad de Química, Universidad Nacional Autónoma de México (UNAM).

(1) Speight, J. G. *The chemistry and technology of petroleum*, 2nd ed.; Marcel Dekker: New York, 1991.

(2) Gruse, W. A.; Stevens, D. R. *The Chemical Technology of Petroleum*; McGraw-Hill: New York, 1960.

(3) Koots, J. A.; Speight, J. G. Relation of petroleum resins to asphaltenes. *Fuel* **1975**, *54* (3), 179−184.

(4) Onogi, S.; Matsumoto, T.; Warashina, Y. Rheological properties of dispersions of spherical particles in polymer solutions. *J. Rheol.* **1973**, *17*, 175−190.

(5) Sengun, M. Z.; Probstein, R. F. Bimodal model of suspension viscoelasticity. *J. Rheol.* **1997**, *41* (4), 811−19.

(6) Werner, A.; Behar, F.; de Hemptinne, J. C.; Behar, E. Viscosity and phase behaviour of petroleum fluids with high asphaltene contents. *Fluid Phase Equilib.* **1998**, *147*, 343−56.

(7) Al-Besharah, J. M.; Salman, O. A.; Akashah, S. A. Viscosity of crude oil blends. *Ind. Eng. Chem. Res.* **1987**, *26*, 2445−2449.

(8) Schorling, P.-C.; Kessel, D. G.; Rahimian, I. Influence of the crude oil resin/asphaltene ratio on the stability of oil/water emulsions. *Colloids Surf. A* **1999**, *152*, 95−102.

(9) El-Gamal, I. M.; Gad, E. A. M. Low temperature rheological behavior of Umbarka waxy crude and influence of flow improver. *Colloids Surf. A* **1998**, *131*, 181−91.

(10) Hodge, I. M. Adam-Gibbs formulation of enthalpy relaxation in glass transition. *J. Res. Natl. Inst. Stand. Technol.* **1997**, *102*, 195−205.

10.1021/ef060159i CCC: $37.00
Published on Web 01/27/2007

temperature. This theory provides the suitable frameworks to express the presence of an activation energy when a transformation occurs, which involves several molecules or several unit segments either of an oligomer or a polymer. Therefore, this theory relates the temperature dependence of the relaxation processes to the temperature dependence of the size of a region, which is defined as a volume large enough to allow cooperative rearrangement to take place without affecting a neighboring region.[10] Cooperative rearrangements are those which require several conformation changes, either of the same oligomer chain or of entangled chains, to be carried out. This cooperatively rearranging region is large enough to allow a transition to a new configuration; hence, it is determined by the polymer chain conformation and, by definition, will equal the sample size at the temperature of solidification of the substance. The transition, in the case of a shear flow, will be from a disordered arrangement typical of liquid to an ordered arrangement, induced by the shear stress. This transition is reflected in the viscous shear thinning region up to reach a Newtonian region, at a shear rate, in which this transition is finished. Besides the Adam−Gibbs theory, it is noteworthy to mention that Bohlin also developed a theory of flow as a cooperative phenomenon.[11]

The oligomer or polymer sample is described as an ensemble of cooperative regions, or subsystems, each containing z^* of unit segments. The transition frequency of such a cooperative rearrangement is then calculated as a function of this subsystem size, to be

$$f(T) = A'_T \exp(-z^*\Delta\mu/RT) \tag{1}$$

where $\Delta\mu$ is the transition state activation energy, A'_T is the frequency factor, whose temperature dependence is usually neglected,[10] T the absolute temperature, and R is the universal gas constant.

The characteristic relaxation time will be

$$k(T) = A_T \exp(z^*\Delta\mu/RT) \tag{2}$$

where A_T is the relaxation time, which can also vary with temperature, e.g., when a phase transition or structure properties are varying. The temperature dependence of z^* is determined by the macroscopic configurational entropy $S_c(T)$:

$$z^* = \frac{N_A s_c^*}{S_c(T)} \tag{3}$$

where N_A is Avogadro's number and s_c^* is the configurational entropy of the smallest number of rearranging molecular entities. Combining eqs 2 and 3, the following equation is obtained:

$$k(T) = A \exp\left(\frac{N_A s_c^* \Delta\mu}{S_c(T)RT}\right) \tag{4}$$

where $S_c(T)$ can be extrapolated by means of the empirical equation for the heat capacity proposed by Van Miltenburg:[12]

$$S_c(T) = \int_{T_o}^{T} \frac{\Delta C_p}{T}\,dT = \frac{(n-1)}{C_o}\int_{T_o}^{T}\left(\frac{b}{T}+c\right)dT = \frac{(n-1)}{C_o}\left[b\ln\frac{T}{T_o} + c(T-T_o)\right] \tag{5.1}$$

$$C_o = b(3-1) + c(3-1)T_o = 2(b + cT_o) \tag{5.2}$$

In eq 5.1, the term ΔC_p is only the configurational term of heat capacity, depending on the number n of carbon atoms of the alkane chain, b and c are constants, C_o is the configurational heat capacity for a polymer segment of 3 carbon atoms, at the reference melting temperature T_o of the considered alkane. The configurational entropy of the corresponding smallest unit, as usually done for polymers,[10] was taken:

$$s_c^* = K_B \ln 2^3 \tag{6}$$

where K_B is Boltzmann's constant and the exponent 3 corresponds to the small polymer segment considered, because it has been demonstrated that this choice shows better results for polymers; thus, z^* is

$$z^* = \frac{N_A s_c^*}{S_c(T)} = \frac{R\ln 2^3}{\frac{(n-1)}{C_o}\left[b\ln\frac{T}{T_o} + c(T-T_o)\right]} \tag{7}$$

This equation shows that the cooperative region size is proportional to the inverse of $n - 1$.

Equation 7 is valid only for linear alkanes and $n \geq 3$. The values of b and c are 13.990 and 0.0543 J K^{-1},[12] respectively.

In Figure 1 is shown the variation of z^* with the inverse of the temperature T (1000/T), for C17, C20, and for *n*-undecane (C11) (in order to show the z^* trend with the variation of carbon atoms), calculated from the equation set of eqs 1−7. It is possible to observe that z^* of C20 is higher than the others and that z^* of C17 is higher than that of C11; in every case, approaching the melting temperature, the z^* values increase dramatically. However, at high temperatures (low 1/T), their values tend to be similar. In Figure 2 is shown the variation of the term $z^*\Delta\mu$, where the trend is similar to that of Figure 1. The value of $\Delta\mu$ was taken as 13 kJ mol^{-1}, which corresponds to an approximated value of the rotational barrier (corresponding to the energy necessary to overcome an *eclipsed* conformation) around a C−C bond, from a stable conformation to another one (*GT* transitions, from *G gauche* conformation to *T trans* conformation). More details on the alkanes' conformation energies can be found in the work of Jaffe.[13] The same values of Figure 2 are reported in Figure 3, but in a logarithmic scale in order to show evidence that C11 at high temperature exhibits a higher $z^*\Delta\mu$ than C17 and C20.

3. Adam−Gibbs Theory Applied to Crude Oil and Blends of Alkanes

In the case of crude oil, where a distribution of alkanes with different numbers of carbon atoms n is present, the calculation of z^* of the mixture is defined as the average $\langle z^*\rangle$ corresponding to the given distribution (molar fraction) of alkanes $X(n)$:

$$\langle z^*\rangle = \sum_{n=1}^{n_{max}} z^*(n)X(n) \approx \int_1^{\infty} z^*(n-1)X(n-1)\,dn \tag{8.1}$$

The passage from a discrete to continuous distribution requires the following condition and, as well, that n_{max} of eq 8.1 (the alkane with longest chain in the specimen) is very great.

(11) Bohlin, L. A theory of flow as a cooperative phenomenon. *J. Colloid Interface Sci.* **1980**, *74* (2), 423−34.

(12) Van Miltenburg, J. C. Fitting the heat capacity of liquid *n*-alkanes, new measurements of *n*-heptadecane and *n*-octadecane. *Thermochim. Acta* **2000**, *343*, 57−62.

(13) Jaffe, R. L. Quantum chemistry study of conformational energies and rotational energy barriers in *n*-alkanes. *J. Phys. Chem.* **1996**, *100* (48), 18718−24.

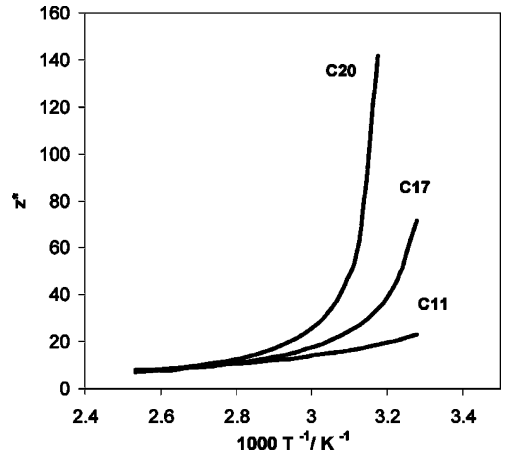

Figure 1. Plot of z^* curves for C11, C17, and C20.

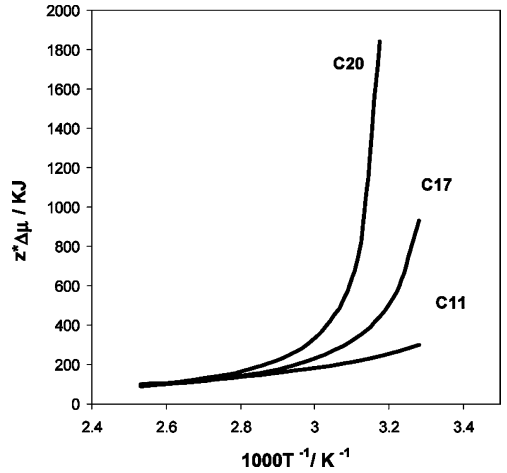

Figure 2. Activation energy vs $1000T^{-1}$ for C11, C17, and C20. The three activation energies tend to be similar at high T.

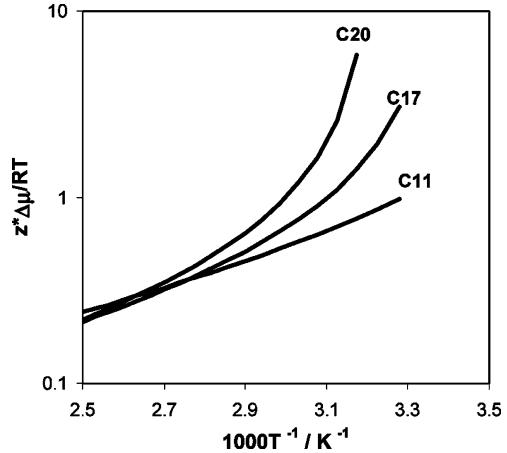

Figure 3. Arrhenius factor vs $1000T^{-1}$ for C11, C17, and C20 in logarithmic scale. It is possible to observe that at high T, the Arrhenius factor of C11 is higher than those of C17 and C20.

Moreover, in order to carry out this approximation, alkanes with great values of n should have molar fractions tending to 0, as occurs in Poisson-like distributions.

$$\int_1^\infty X(n-1)\,\mathrm{d}n = 1 = \sum_{n=1}^{n_{\max}} X(n) \tag{8.2}$$

Where in eqs 8.1 and 8.2, $X(n-1)$ substitutes $X(n)$ to simplify calculations and $z^*(n)$ is the z^* of the alkane with n carbon atoms. The Poisson distribution is similar to alkanes' distribution in crude oil, as evidenced by the work of Musser and Kilpatrick;[14] indeed, it is a very common distribution in natural phenomena as in chemical kinetics, etc. Nevertheless, the conclusions do not depend on the kind of the utilized distribution. The central idea is that the alkane with the maximum molar fraction is different form the average alkane chain. As in most cases of both natural and artificial mixtures, there is an excess component and a different average. Therefore, if we suppose that we have a Poisson distribution of alkanes in the complex mixture of real oil, the following expression can be used:

$$X(n-1) = \lambda^2(n-1)\exp[-\lambda(n-1)] \tag{9}$$

which satisfies eqs 8.1 and 8.2; λ is called the frequency factor in a Poisson distribution. It is easy to show that the average $\langle z^* \rangle$ is given by the following:

$$\langle z^* \rangle = \int_1^\infty X(n-1)\frac{N_A s_c^*}{S_c(T)}\,\mathrm{d}n = \int_1^\infty \frac{\lambda^2(n-1)\exp[-\lambda(n-1)]R\ln 2^3}{\frac{(n-1)}{\xi_o}\left[b\ln\frac{T}{\theta_o} + c(T-\theta_o)\right]}\,\mathrm{d}n = \frac{\lambda R\ln 2^3}{\frac{b}{\xi_o}\ln\frac{T}{\theta_o} + \frac{c}{\xi_o}(T-\theta_o)} \tag{10}$$

In eq 10, it is shown that $\langle z^* \rangle$ depends on three parameters, λ, ξ_o, and θ_o. The inverse of λ is $N-1$ which corresponds to the maximum $n-1$ of the proposed Poisson distribution, as inferred by deriving eq 9:

$$N - 1 = \frac{1}{\lambda} \tag{11.1}$$

Thus, eq 10 can be written in a form quite identical to eq 7 but with the explicit linkage between the average z*, $\langle z^* \rangle$, with the maximum $n-1$, $N-1$.

$$\langle z^* \rangle = \frac{R\ln 2^3}{\frac{(N-1)}{\xi_o}\left[b\ln\frac{T}{\theta_o} + c(T-\theta_o)\right]} \tag{11.2}$$

The parameter ξ_o corresponds to C_o (eq 5.2) calculated for the temperature θ_o. Otherwise, θ_o is a parameter substituting the melting temperature.

In eq 10, θ_o has no more physical significance of the melting temperature of a pure compound and is given by the substitution of n with N in the following equation:

$$T_{on} = 1635.5 + 2971(n-1)^{0.1428} - 4460(n-2)^{0.05842} - 236.7(n-3)^{0.3554} - 0.01762(n-4)^{2.727} + 16.11\left\{\frac{(n-1)n(n+1)}{6}\left[\frac{\Gamma(n+1)}{2\Gamma(n-1)}\right]^{-1}\right\}^{1.047} \tag{12}$$

This equation[16] predicts the melting points of normal alkanes with a number of carbon atoms n in the range 8−25. T_{on} is the melting of the pure alkane with n carbon atoms. In Figure 4,

(14) Musser, B. J.; Kilpatrick, P. K. Molecular characterization of wax isolated from a variety of crude oil. *Energy Fuels* **1998**, *12*, 715−25.

(15) Burch, K. J.; Whitehead, E. G., Jr. Melting-Point models of alkanes. *J. Chem. Eng. Data* **2004**, *49*, 858−863.

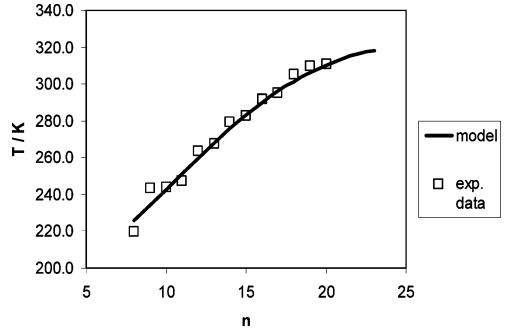

Figure 4. Melting points of *n*-alkanes: (solid curve) model prediction; (boxes) experimental values.[12,15]

the accuracy of this equation is shown. The gamma function, Γ, is used to avoid the use of the factorial function, because *N* is not generally an integer value since it is calculated by eq 11.1. Moreover, eq 12 is derived from the model proposed by Burch and Whitehead,[15] and it is suitable to predict the melting points of both pure linear and branched alkanes.

If a physical sense can be attributed to the temperature θ_o, although it is taken as the melting temperature of the alkane with *N* carbon atoms, it cannot correspond to the melting temperature of a pure compound, but more probably to a transition temperature of a mixture of several compounds, in which the behavior of the alkane in excess prevails. This excess alkane contributes significantly to the interlocking lattice of wax crystals of the crude.

The average $n - 1$ is exactly the double of the maximum:

$$\langle n - 1 \rangle = \frac{2}{\lambda} \tag{13}$$

The choice to use the transition temperature of the excess alkane as the reference temperature θ_o of eq 11.2, is in accordance with experimental results, as shown ahead in sections 5 and 6. This fact confirms the idea that the excess alkane, with *N* carbon atoms, should be involved in the building of wax networks,[16] and its melting should weaken this structure.

4. General Rheological Model for Shear Thinning Fluids Applied to Alkanes and Crude Oils

The model adopted for both the crude oil and alkanes for shear thinning behavior is the same described in detail and proposed by Al-Zahrani:[17] a three parameter equation of *power-law* type,

$$\eta(\dot{\gamma}) = B\left[\left(\frac{\dot{\gamma} + A}{\dot{\gamma}A}\right)^p - \frac{1}{\dot{\gamma}^p}\right]^{1/p} \tag{14}$$

where $\dot{\gamma}$ is the shear rate, *A* has dimensions of shear rate, *B* has dimensions of stress, the ratio *B/A* is the viscosity at shear rates tending to infinity, and *p* is an exponent, which is related to molecular weight. In Table 1, the values of *A*, *B*, and *p* are reported for both the considered oil and the utilized *n*-heptadecane/*n*-eicosnane mixture. The specimens of the considered crude oil are from a sample of the Cantarell reservoir. It is noteworthy to observe that the same model works well enough for mixtures of alkanes and the considered oil. The rheological tests were carried out by a strain controlled rheometer ARES (advanced rheometric expansion system). The same cone−plate geometry was used for all the tests with an angle of 0.04 radians and a plate radius of 50 mm.

Table 1. Values of *A* and *B* for Crude Oil and the C17/C20 Mixture with a Molar Fraction of 0.16 in C20

	A (s^{-1})	B (dyne cm^{-2})	p
crude oil (293 K)	3.98×10^{-2}	29	4.2
crude oil (305 K)	9.4×10^{-2}	19	4.2
C17/C20 mixture (305 K)	37.51	1.12	18

Previous research demonstrated that a Weissenberg number[18,19] scales the shear rate at different temperatures for the crude oil considered and mixtures of alkanes.

This Weissenberg number was so defined:

$$We = k\,\dot{\gamma} = k_0 \exp(\epsilon/RT)\dot{\gamma} = \frac{\dot{\gamma}}{\dot{\gamma}_c} = \dot{\gamma}' \tag{15}$$

where *k* and k_0 are constants with time dimensions and ϵ is the activation energy. Moreover, $\dot{\gamma}_c$ and η_c are defined as the critical shear rate and the critical viscosity, respectively, i.e., the shear rate and viscosity which correspond to the crossing point of the straight line extrapolated by the linear shear thinning region with the straight line extrapolated by the Newtonian region. In other words, they are the viscosity and shear rate corresponding to the transition from the shear thinning region to the subsequent Newtonian region. This point and the method used to find the critical viscosities and shear rates are discussed in detail in the previous paper by Dante et al.[18] On the other hand, the viscosity is scaled by the inverse of the critical viscosity η_c:[19−21]

$$\eta' = h'\eta = h_0 \exp(-\epsilon/RT)\eta = \frac{\eta}{\eta_c} = \eta' \tag{16}$$

where h' and h_o are constants with dimensions of the inverse of viscosity. Since eqs 15 and 16 have a very similar form to eqs 1 and 2, the activation energy ϵ can be interpreted in this form:

$$\epsilon = z^*\Delta\mu \tag{17}$$

Nevertheless, in this form, ϵ will be not a constant, implying that also h_0 and k_0 will be not constant. The difficulty of managing eq 16 in terms of the Adam−Gibbs theory consists in the uncertainty of the factors k_0 and h_0. However, this obstacle can be overcome by utilizing the model of eq 14 for a specific temperature as starting and reference point. The Adam−Gibbs theory has been introduced because it gives a physical explanation to the observed activation energy. Indeed, the activation energies found for crude oil and the studied alkanes' mixtures stay in the range of 70−20 kJ mol^{-1} for the considered range of temperature 295−340 K,[18] which are very similar to the activation energies determined by the application of the Adam−Gibbs theory.

In spite of the analogy between the equations' forms, second, there is a deep analogy among values and, finally, the capacity of the models derived from the theory to predict the experimental

(16) Kioupis, L. I.; Maginn, E. J. Rheology, dynamics, and structure of hydrocarbon blends, a molecular dynamics study of n-hexane/n-hexadecane mixtures. *Chem. Eng. J.* **1999**, *74*, 129−46.

(17) Al-Zahrani, S. M. A generalized rheological model for shear thinning fluids. *J. Pet. Sci. Eng.* **1997**, *17*, 211−5.

(18) Dante, R. C.; Geffroy-Aguilar, E.; Chávez, A. E. Viscoelastic models for Mexican heavy crude oil and comparison with a mixture of heptadecane and eicosane. Part I. *Fuel* **2006**, *85* (4), 559−68.

(19) Miadonye, A.; Puttagunta, V. R.; Singh, B. Prediction of the viscosity of crude oil fractions from a single measurements. *Chem. Eng. Commun.* **1993**, *122*, 195−9.

(20) Al-Zahrani, S. M.; Al-Fariss, T. F. A general model for the viscosity of waxy oils. *Chem. Eng. Process.* **1998**, *37*, 433−7.

(21) Pal, R. Scaling of relative viscosity of emulsions. *J. Rheol.* **1997**, *41*, 141−50.

values. Other equations can be used such as the WLF (Williams-Landel-Ferry) equation,[22] probably arriving to similar conclusions; although, emphasis is given to free volume. Nevertheless, the free volume concept and cooperative regions should be correlated.

At the selected temperature, e.g., $T_1 = 293$ K, we can use eq 15 and obtain $\dot{\gamma}'$ through $\dot{\gamma}_c$. From our definition, $\dot{\gamma}'$ defines the dimensionless shear rate at different temperature. At the temperature T_2, the following equations are valid:

$$\dot{\gamma}' = A_{T_2} \exp(z^*\Delta\mu/RT_2)\dot{\gamma}_{T_2} = \frac{\dot{\gamma}_{T_1}}{\dot{\gamma}_{cT_1}} \tag{18}$$

$$\dot{\gamma}_{T_2} = \dot{\gamma}_{T_1}\left(\frac{A'_{T_2}}{\dot{\gamma}_{cT_1}}\right) \exp(-z^*\Delta\mu/RT_2) \tag{19}$$

This implies that $A'_{T_2}/\dot{\gamma}_{cT_1}$ is the parameter used to fit experimental viscosity curves.

The viscosity at the temperature T_2 is obtained in the following way:

$$\eta_{T_2} = \eta_{T_1}\left(\frac{\sigma_{cT_1}A_{T_2}}{\eta_{cT_1}}\right) \exp(z^*\Delta\mu/RT_2) = \eta_{T_1}(\dot{\gamma}_{cT_1}A_{T_2}) \exp (z^*\Delta\mu/RT_2) \tag{20}$$

Where, σ_{cT_1} is the critical shear stress at T_1. In this case, the parameter is $\dot{\gamma}_{cT_1}A_{T_2}$, and it is noteworthy that

$$\dot{\gamma}_{cT_1}A_{T_2} = \left(\frac{A'_{T_2}}{\gamma_{cT_1}}\right)^{-1} \tag{21}$$

which implies that

$$\eta_{T_2}\dot{\gamma}_{T_2} = \eta_{T_1}\dot{\gamma}_{T_1} \tag{22}$$

and closes the loop leading us to the well-known equation for the viscosity function:

$$\eta(\dot{\gamma}) = \frac{\sigma(\dot{\gamma})}{\dot{\gamma}} \tag{23}$$

Finally, we remind that

$$h_0 = \frac{1}{A_T\sigma_{cT}} \tag{24.1}$$

$$k_0 = A_T \tag{24.2}$$

In eqs 24.1 and 24.2, the idea that both k_0 and h_0 are not constant is expressed.

The strategy displayed by eqs 15−21 allowed us to reproduce the viscosity curves of the mentioned oil and the mixture of alkanes.

5. Application of the Model to a Mixture of *n*-Heptadecane and *n*-Eicosane

In an artificial binary mixture of alkanes, the molar fractions are known and it is not necessary to suppose the kind of distribution, as in the general case of a crude oil sample.

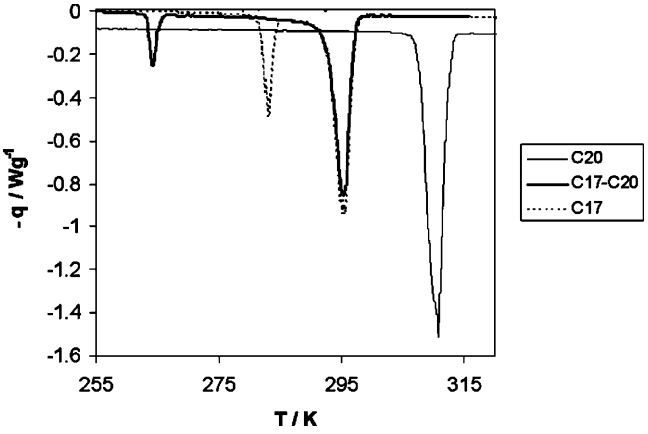

Figure 5. DSC curves for C20, the C17−C20 mixture, and C17.

In this case, the molar fractions of heptadecane and eicosane were as follows:

$$X(17) = 0.84$$
$$X(20) = 1 - X(17) = 0.16 \tag{25}$$

The chosen values are just used as an example of how the Adam−Gibbs theory works with alkanes. Heptadecane was chosen as the excess alkane for its lower melting point, allowing us to prepare blends at room temperature. If the assertions of section 3 are accepted, which say that the behavior of the component with the maximum molar fraction prevails, the melting temperature of the *n*-heptadecane, taken as 295.9 K and calculated by eq 12, was the value assigned to θ_o in eq 11.2. In this case, the average *n* is 17.5, not far from the maximum 17, but which would imply a melting temperature of 305.8 K, utilizing eq 12.

Differential scanning calorimetry (DSC) was carried out using a calorimeter of TA instruments, model 2910. The DSC curves of the mixture, of pure heptadecane (C17), and of pure eicosane (C20) are shown in Figure 5. The melting temperature of C17 is 295.4 K (295.9 K, calculated by eq 12), and the melting point of C20 is 310.6 K (310.3 K, calculated by eq 12), as obtained from these data. The experimental data and the eq 12 model show good agreement. The phase concerning the transition of C17 is the so-called rotator phase, and the phase of C20 is the triclinic phase. It is useful to remind that even and odd alkanes have different solid phases and exhibit polymorphism; more information on the subject can be found in the paper of Rajabalee et al.[23] The transition temperature for the mixture is 295.5 K, very close to the melting point of pure C17. In the mixture, the peak of the solid−solid phase transition present in pure C17 is shifted from 283 to 264 K (Figure 5).

The melting heat is 73.3 kJ mol^{-1} for C20, 43.9 kJ mol^{-1} for C17, and 38.7 kJ mol^{-1} for the mixture.

These results confirm that the transition temperature of the mixture is very close to that of C17.[23]

In Figure 6, the viscosity curves of the mixture are shown at three different temperatures.[18] It is possible to reproduce these curves applying the considerations of section 4, supposing that the experimental results are determined by the prevailing C17 behavior, as settled by eq 11.2. The results are exposed in Figure 7a. In order to fit the experimental curves, the parameter A_T has to vary with temperature. However, the effect of temperature on the viscosity curves is low, due to the combination of low

(22) Ferry, J. D. Dependence of viscoelastic behavior on temperature and pressure. In *Viscoelastic properties of polymers*; John Wiley & Sons, Inc.: New York, 1980; Chapter 11, pp 264−320.

(23) Rajabalee, F.; Metvaud, V.; Oonk, H. A. J.; Modieig, D.; Waldner, P. Perfect families of mixed crystals, the "ordered" crystalline forms of n-alkanes. *Phys. Chem. Chem. Phys.* **2000**, *2*, 1345−50.

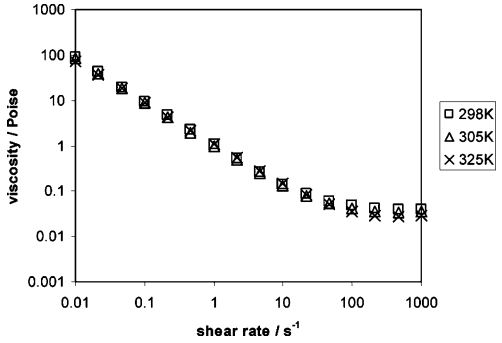

Figure 6. Viscosity curves of the C17/C20 mixture at different temperatures: 298, 305, and 325 K.

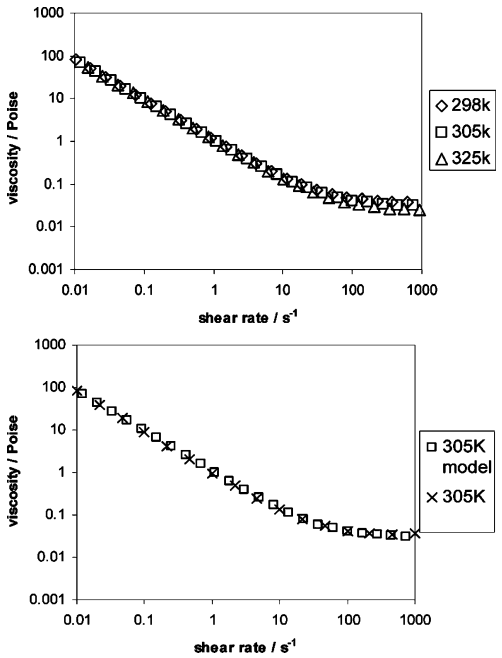

Figure 7. (a) Model predictions of the viscosity curves of the C17/C20 mixture at different temperatures: 298, 305, and 325 K. (b) Comparison between the viscosity obtained by model prediction at 305 K (square box curve) and the experimental viscosity of the C17/C20 mixture at the same temperature (cross curve).

z^* and the low variation of the relaxation time A_T of this mixture (between 1 and 8 s) in the considered range of temperature 298−325 K.

Indeed, the viscosity at 464 s^{-1} passes from 3.9×10^{-2} P at 298 K to 2.6×10^{-2} P at 325 K (Figure 6). Moreover, the viscosity curves tend to be very similar at low shear rates. At high shear rates, where the effect of the temperature should be stronger, the decay of the viscosity in not very pronounced (Figure 6). The direct comparison between the experimental viscosities of the mixture at 305 K and the model curve at the same temperature is reported in Figure 7b. The overlap of the curves is quite good in this case.

6. Application of the Model to the Crude Oil Sample

The DSC analysis of the crude oil sample has not shown a specific transition of the first order that can be associated to any kind of phase change of paraffins (Figure 8), in the range of temperature of 290−320 K.[14] The viscosity curves are reported in Figure 9. In this case, the effect of the temperature is stronger than in the alkanes' case, as it can be inferred by the decay of viscosity at the shear rate of 2.15 s^{-1}: from 860 P at 293 K to 29 P at 333 K.

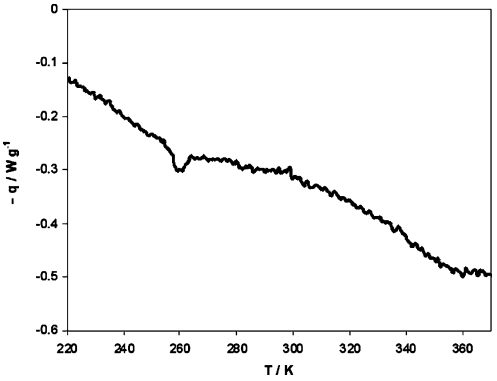

Figure 8. Crude oil specimen DSC curve.

In Figure 10a, the results of the model exposed, taking the maximum $N = 20$ (eq 11.1), are shown. The choice of $N = 20$ is based upon certain evidences given here in succession. The thermal gravimetric analysis (TGA) of crude oil, carried out by means of a TGA 2950 of TA instruments in N_2 flux (Figure 11), reveals a region between 340 and 640 K where aliphatic compounds are the principal cause of weight loss. The TGA derivative curves overlapped of crude oil, C11 and C20, reveal that C20 is placed approximately in the middle of this region-as the maximum N should stay-, while C11 is placed on the left side, meaning that the low molecular weight components are not abundant (Figure 12).

The comparison between experimental viscosity functions at 293 and 333 K with model curves at the same temperatures is directly presented in Figure 10b. Good overlaps of the curves can be observed. The variation of A_T is very pronounced (Figure 13), revealing a transition next to 311 K ($1000/T = 3.2$ K^{-1}), similar to the transition of C20 from the triclinic phase to the liquid phase. Since a transition was not observed by DSC, the rheological data were studied in order to find a signal of a possible transition; for this reasons, the analyses of both shear and normal stresses were considered. A relaxation time τ is obtained directly by the first coefficient of normal stresses at the shear rate of 0.2 s^{-1}, which exhibits a significant variation at about 313 K (Figure 14) and can be compared with A_T. In Figure 14, τ is normalized by means of τ at 293 K.

$$\tau = \frac{2\eta}{\psi_1} \tag{26}$$

In eq 26, the relaxation time τ is expressed; η is the viscosity, and ψ_1 the first coefficient of normal stresses. From the thermodynamic point of view, stress can be considered as the derivative of the Helmoltz free energy F with respect to volume V at constant T. The shear stress, at the critical shear rate, has a transition at about 312 K (Figure 15), in accordance with the prediction of the model.

7. Discussion

The Adam−Gibbs theory can provide some explanation for the Arrhenius factor found in waxy crude oil and the very pronounced shear thinning. Alkanes or alkylic chains seem to determine the main features of viscosity properties of the crude oil sample. The higher absolute value of the viscosity of crude oil (Figure 9) depends upon the complex interactions among its components. In our case, aliphatic components, among them alkanes, surround the dispersed particles composed of wax, and asphaltenes. Changes in their organization induced by flow[24] cause the appearance of the activation energy defined in the

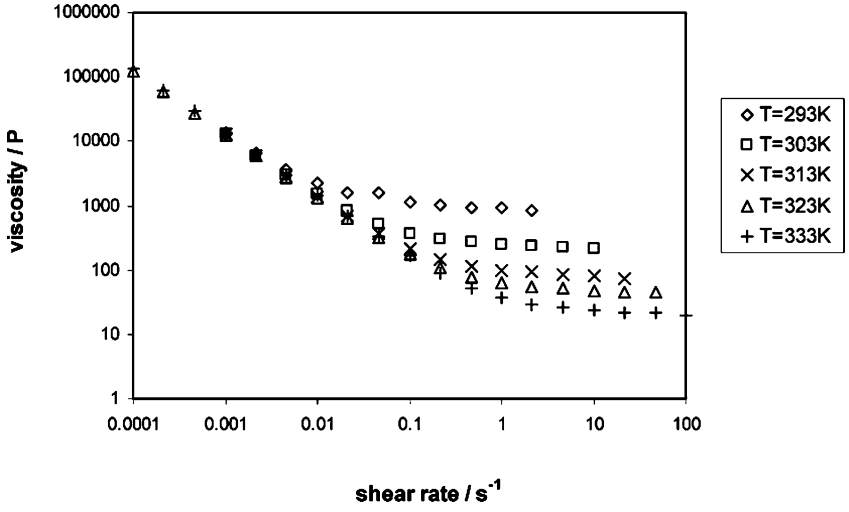

Figure 9. Crude oil viscosity curves in the temperature range 293−333 K.

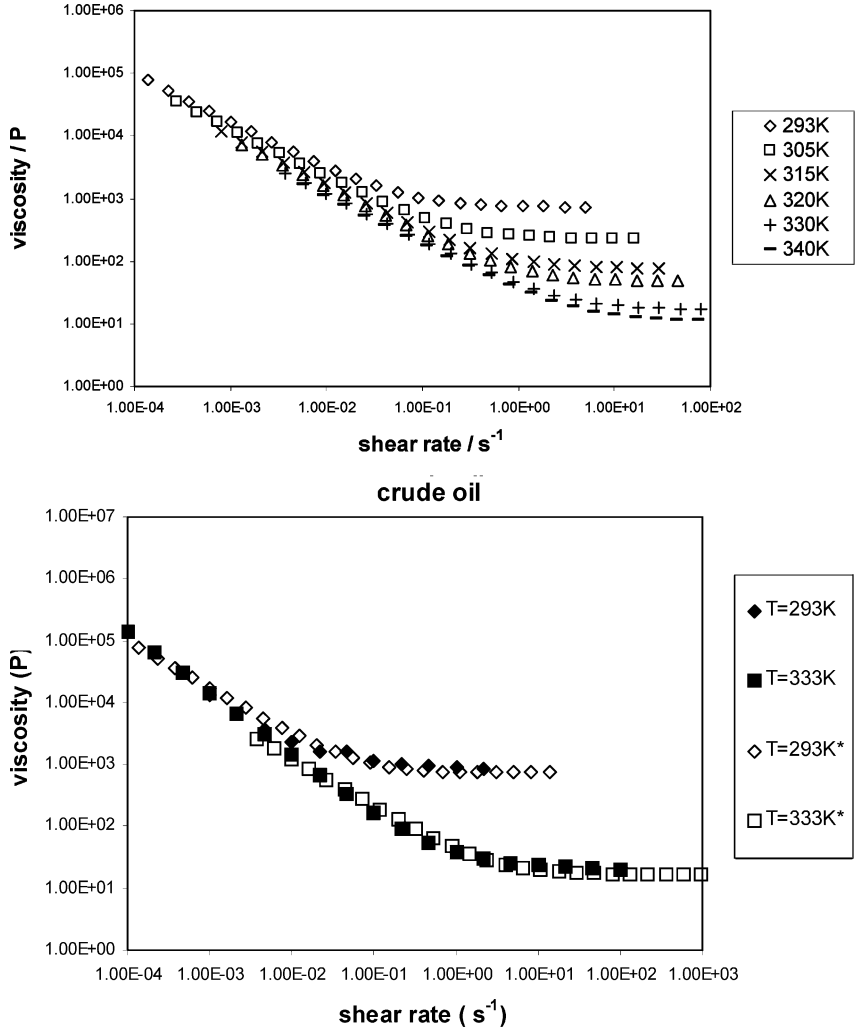

Figure 10. (a) Model prediction of the crude oil viscosity curves in the temperature range 293−340 K. (b) Comparison among experimental curves at 293 and 333 K (curves with bold boxes) and model curves at the same temperatures (curves with empty boxes).

Adam−Gibbs theory (eqs 1−11.2). An example of conformation change of alkane chains is shown in Figure 16 for *n*-eicosane. Polymer phase changes implicate reorganization of large regions that are interconnected and tangled. Elemental segments have to change their conformation by means of rotations and torsions, to which an energy barrier is associated and called $\Delta\mu$. The cooperative region z^* varies with temperature and chain length, i.e., with the number of carbon atoms n. Longer chains have larger z^* values, and when the transition temperature is approached, z^* increases dramatically, because the cooperative region takes the limit size of the whole solid. It is noteworthy

(24) Pricl, S.; Fermeglia, M. Virtual rheological experiments on linear alkane chains confined between titanium walls. *Rheol. Acta* **2001**, *40*, 104−10.

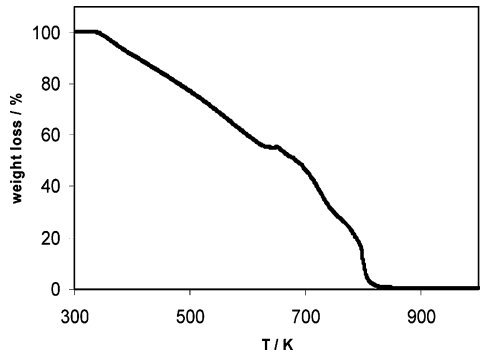

Figure 11. TGA weight loss percentage for the crude oil sample in the range of 300−1000 K in N_2 flux.

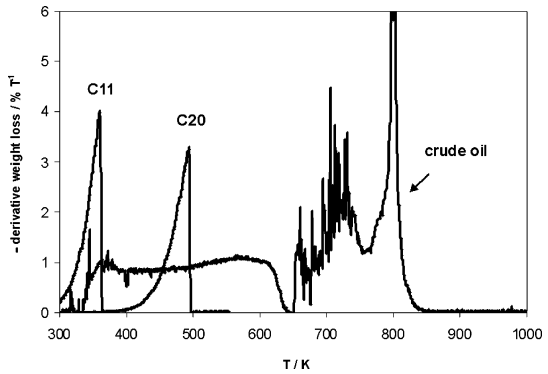

Figure 12. Derivatives of the TGA curves of the crude oil sample, C11, and C20 in N_2 flux.

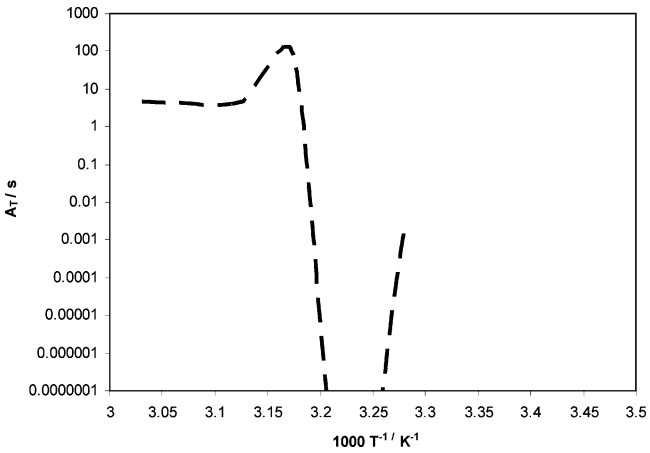

Figure 13. A_T variation as obtained by the model for crude oil.

to mention that the cooperative region size depends on the maximum N and not on the average $\langle n \rangle$. The size of z^* determines the activation energy, which is not a true constant. The relaxation time $k(T)$ increases with z^*, while A_T can be interpreted as the extrapolation of the limit case of $k(T)$ at high T. Nevertheless, it depends on temperature, because it is sensitive, e.g., either to the presence of suspended particles or to changes of fluid structures, which also affect relaxation time. This should be the reason that there is a very abrupt change, which follows the aliphatic transition at about 310 K for crude oil (Figure 13). The transition in the C17−C20 mixture can be observed by DSC, and it is found very close to the C17 transition, $T = 295.5$ K (Figure 5). On the other side, no clear transitions are observed in crude oil by DSC (Figure 8) near the expected region (∼310 K); there can be two reasons for this: the former says that it can be too small or broad to be

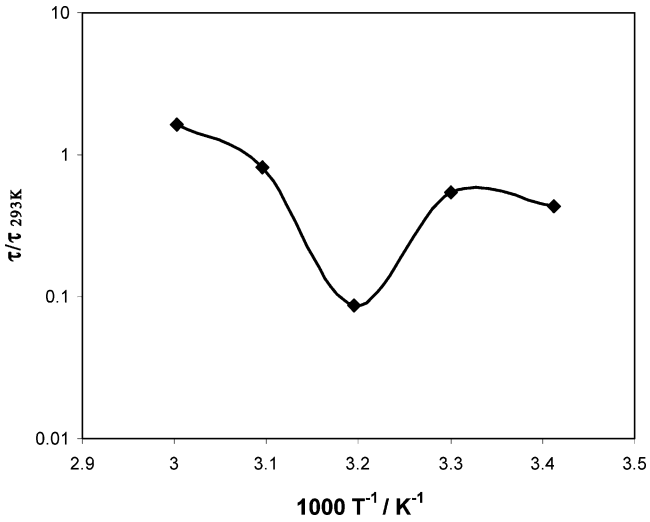

Figure 14. Relaxation time τ normalized to τ at 293 K and referred to the shear rate of 0.2 s^{-1}. This relaxation time is calculated through the first coefficient of normal stresses ψ_1 (eq 26).

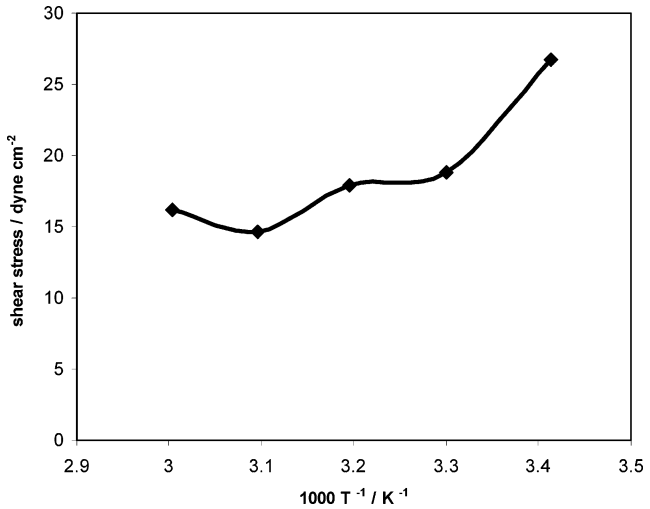

Figure 15. Shear stress at the critical shear rate $\dot{\gamma}_c$ defined in section 4.

detected, and the latter would imply that it is a second-order transition. Moreover, it is well-known in the oil industry that crude oil does not undergo first-order transitions. A second-order transition implies an aliphatic network more similar to a gel than to a solid. Some transitions of alkane binary mixtures are shifted largely (from 283 to 264 K in our case), although others, dominated by the excess alkane, are kept mostly unvaried. However, the rotator phase seems to be more stable and dominated by the excess alkane C17. The shifted and lowered peak of the solid−solid transition (Figure 5) is due to the fact that this phase is weakened by the presence of the even alkane (C20).[23]

The application of the Adam−Gibbs theory to viscosity functions is described in section 4. The experimental viscosity curves of Figure 6 for the alkanes' mixture and Figure 9 for the crude oil can be reproduced taking into account the activation energy expressed by the Adam−Gibbs theory. The central role is played by the shear thinning model of eq 14, which describes both alkane blends and the considered oil. The two parameters A and B can be made dimensionless by means of the Weissenberg number of eq 15 and by η' of eq 16, respectively. The parameter p is often not reproducible, indicating that its variation

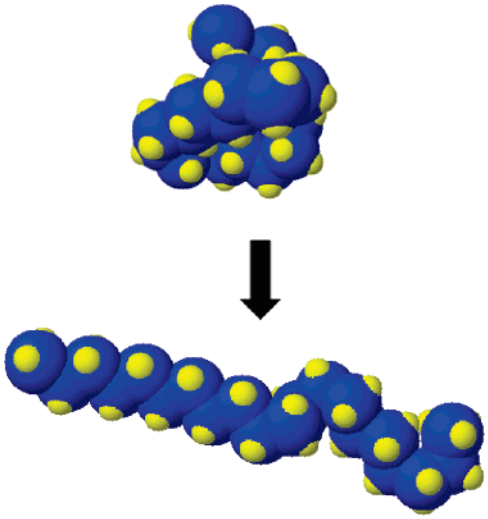

Figure 16. Two different conformations of C20. The upper conformation is "ball-shaped" and the lower one is "snakelike". An energy barrier, which involves the rotation barrier of C−C bonds, must be overcome to pass from one to another.

not only depends on molecular weight but also on other factors such as the state of the sample before test.[11] However, it could be made dimensionless through the average $\langle n \rangle$.

Summing up, the effect of temperature would be manifested through N and the effect of shear forces through $\langle n \rangle$.

8. Conclusions

The exposed results show that the considered crude oil, with a high content of aliphatic compounds, and the blends of alkanes obey an identical system of phenomenological rheological equations (eqs 14−22). This means that the rheological properties of crude oil are determined overall by alkanelike compounds such as paraffins and compounds with a relevant alkylic chain.

The Adam−Gibbs theory[10] explains quite well the relaxation time variation occurring in polymers and can explain the arising of variable activation energy. Combining this characteristic time with shear rate, a Weissenberg number (eq 15)[18] is obtained, capable of scaling both alkane and crude oil viscosities. The cooperative region size z^* (eq 11.2), which varies depending on the number of carbon atoms of the excess alkanes, can also explain the arising of different activation energies in different blends. These analogies allow us to bypass the complexity of crude oil composition and to correlate its rehological properties to those of more simple and reproducible systems such as alkanes' mixtures.[18] The rheological differences between oil and alkanes depend essentially on the cooperative changes induced by flow and temperature. Although, the Adam−Gibbs theory provides a common framework to the mechanisms which cause the appearance of the activation energy, there are substantial differences.[1−3] In crude oil, the extent of changes is deeper than in the alkanes' mixture, as evidenced by the variation of both the viscosity (Figure 9) and the relaxation time A_T (Figure 13) with temperature. This is due mainly to the fact that in the case of alkanes' blends we are working above their transition temperature; thus, only the tail end of the phenomenon is observed. In this case, working while the transition occurs is impossible, because we would have a solid specimen. The transition occurring in crude oil cannot be clearly observed by DSC (Figure 8), but is evidenced by shear stress and relaxation time changes in the proximity of the expected transition temperature (see Figures 14 and 15). However, as expected by Adam−Gibbs theory, above the transition temperature, the effect of the activation energy $z^*\Delta\mu$ is faded.

EF060159I